



Enhancement of snow albedo reduction and radiative forcing due to coated black carbon in snow

Wei Pu¹, Tenglong Shi¹, Jiecan Cui¹, Yang Chen¹, Yue Zhou¹, and Xin Wang^{1,2}

¹Key Laboratory for Semi-Arid Climate Change of the Ministry of Education, College of Atmospheric Sciences, Lanzhou University, Lanzhou 730000, China

²Institute of Surface-Earth System Science, Tianjin University, Tianjin 300072, China

Correspondence: Xin Wang (wxin@lzu.edu.cn)

Received: 14 August 2020 – Discussion started: 2 September 2020

Revised: 15 March 2021 – Accepted: 22 March 2021 – Published: 17 May 2021

Abstract. When black carbon (BC) is mixed internally with other atmospheric particles, the BC light absorption effect is enhanced. This study explicitly resolved the optical properties of coated BC in snow based on the core/shell Mie theory and the Snow, Ice, and Aerosol Radiative (SNICAR) model. Our results indicated that the BC coating effect enhances the reduction in snow albedo by a factor ranging from 1.1–1.8 for a nonabsorbing shell and 1.1–1.3 for an absorbing shell, depending on the BC concentration, snow grain radius, and core/shell ratio. We developed parameterizations of the BC coating effect for application to climate models, which provides a convenient way to accurately estimate the climate impact of BC in snow. Finally, based on a comprehensive set of in situ measurements across the Northern Hemisphere, we determined that the contribution of the BC coating effect to snow light absorption exceeds that of dust over northern China. Notably, high enhancements of snow albedo reduction due to the BC coating effect were found in the Arctic and Tibetan Plateau, suggesting a greater contribution of BC to the retreat of Arctic sea ice and Tibetan glaciers.

1 Introduction

Snow is the most reflective natural substance on the surface of Earth and covers more than 30 % of the global land area (Cohen and Rind, 1991). Snow albedo feedback is considered one of the major energy balance factors of the climate system. Previous observations have revealed that light-absorbing particles (LAPs; e.g., black carbon (BC), organic carbon (OC), and mineral dust) within snow may reduce

snow albedo and enhance the absorption of solar radiation (Hadley and Kirchstetter, 2012). As a result, LAPs play a major role in the alteration of snow morphology and snowmelt processes and therefore yield important effects on local hydrological cycles and global climate (Qian et al., 2009).

Given the importance of the climate feedback caused by LAPs in snow, studies have developed snow radiative models and sought to improve our understanding of the influence of LAP-contaminated snow on climate. For example, Warren and Wiscombe (1980) developed a radiative forcing model based on the Mie theory and the δ -Eddington approximation and reported that snow albedo at visible wavelengths could be reduced by 5 %–15 % with 1000 ng g^{−1} BC in snow. Flanner et al. (2007) established a more comprehensive snow albedo model (the Snow, Ice, and Aerosol Radiation model, SNICAR) for a multilayer snowpack based on the two-stream radiative transfer solution. In addition to BC, the SNICAR model also considers the potential effects of dust particles and volcanic ash on snow albedo. Recently, studies have indicated that the mixing state of BC and snow could effectively alter snow albedo (Liou et al., 2011, 2014; Flanner et al., 2012; Liu et al., 2012; He et al., 2017, 2018a, b, c). Moreover, the snow grain shape exerts an important influence on snow albedo (Kokhanovsky and Zege, 2004). Non-spherical snow grains attain a lower albedo reduction than that due to spherical snow grains (He et al., 2018c; Dang et al., 2016).

Although efforts have been made to optimize snow albedo models, current models still suffer from major limitations. Studies have demonstrated that when BC in the atmosphere is coated with other aerosols, this greatly enhances light ab-

sorption via a lensing effect over uncoated BC, as investigated via model simulations (e.g., Jacobson 2001; Matsui et al., 2018) and experimental measurements (e.g., Cappa et al., 2012; Peng et al., 2016). Moreover, coated BC has been observed to persist for only a few hours after emission in certain regions (Moteiki et al., 2007; Moffet and Prather, 2009). Global aerosol models that simulate microphysical processes have revealed that most BC is mixed with other particles within 1–5 d (Jacobson, 2001) at all altitudes (Aquila et al., 2011). However, it remains uncertain whether coated BC occurs in real snowpacks because the coating materials (e.g., salts and OC) other than BC may dissolve during wet deposition. A recent study observing the individual particle structure and mixing states between glaciers–snowpacks and the atmosphere based on field measurements and laboratory transmission electron microscopy (TEM) and energy dispersive X-ray spectrometry (EDX) instrument analysis (Dong et al., 2018) has provided an answer. It was found that salt-coated BC was still observed in real snowpacks despite its lower proportion than that in the atmosphere due to the dissolution effect during snow precipitation. Regarding OC, the above study did not observe reduced OC components in LAPs. More notably, it was also determined that the proportion of coated BC was even higher in snowpacks than that in the atmosphere. All of the above observation results demonstrate that coated BC particles occur in real snowpacks and are even more common than those occurring in the atmosphere. Hence, the climate impacts of BC must be evaluated within the context of the BC coating effect on light absorption enhancement.

Although the BC coating effect on light absorption enhancement in the atmosphere has been broadly acknowledged, little research has been carried out on snow albedo. Flanner et al. (2007) developed the first radiative transfer model to investigate the coating effect on snow albedo, thereby employing sulfate as BC particle coating material with a constant absorption enhancement factor of ~ 1.5 . Subsequently, Wang et al. (2017) considered a similar constant light absorption enhancement factor in their spectral albedo model for dirty snow (SAMDS). However, the above factor varies with the optical properties of different coating materials, core / shell ratio, wavelength, and other parameters in real environments (Lack and Cappa, 2010; Liu et al., 2017). For example, Liu et al. (2017) reported that the core / shell ratio notably controls light absorption enhancement. You et al. (2016) suggested that light absorption enhancement is highly correlated with visible or near-infrared (NIR) wavelengths and coating material. Furthermore, a core / shell Mie-theory-based simulation study (Lack and Cappa, 2010) found that the attained light absorption enhancement was smaller for mildly absorbing coatings (e.g., OC) than that attained for nonabsorbing coatings (e.g., sulfate). Hence, the use of a constant enhancement factor may result in biased simulation estimates, which prevents us from obtaining a better under-

standing of the hydrological and climate impacts of BC in snow.

In this study, we apply the core / shell Mie theory to calculate the optical properties of coated BC considering both mildly absorbing OC and nonabsorbing sulfate and incorporate these results into the SNICAR model to evaluate the influence on snow albedo. Parameterizations of the BC coating effect are then developed for application in other snow albedo and climate models. Finally, we estimate the enhancement of snow albedo reduction and the associated radiative forcing due to the BC coating effect across the Northern Hemisphere by combining model simulations with in situ observations of the BC and OC concentrations in snow.

2 Methods

2.1 Modeling

2.1.1 Optical parameter calculations for snow coated in BC

Figure 1a and 1c show schematics of light absorption by externally and internally mixed particles (EMPs and IMPs, respectively). EMPs are particles not coated in BC mixed with other particles, while IMPs include BC, which is assumed to be the core material coating particles and acts as a shell (Kahnert et al., 2012). Regarding the nonabsorbing shell, the overall light absorption includes contributions of the BC core and absorption enhancement due to the lensing effect, while regarding the absorbing shell, the shell itself also contributes to light absorption. The lensing effect indicates that when BC is coated with a nonabsorbing shell (or an absorbing shell), the shell acts as a lens and focuses more photons onto the core than would reach it otherwise so that the light absorption effect of the BC core is enhanced (Bond et al., 2006).

To evaluate the BC coating effect on snow albedo, it is necessary to determine the optical parameters of coated BC. The refractive index (RI) of BC was assumed to be $1.95-0.79i$ following Lack and Cappa (2010), which is consistent with the original SNICAR model (Flanner et al., 2007). Two types of particle shells (nonabsorbing and absorbing) were considered. The nonabsorbing shell was represented with sulfate, and its RI was set to be $1.55-10^{-6}i$ following the atmospheric study of Bond et al. (2006). The absorbing shell was represented with OC, which is a major light-absorbing particle in snow (Wang et al., 2013). The RI of OC varies with the wavelength. Here, a fixed mass absorption coefficient (MAC) for OC of $0.3 \text{ m}^2 \text{ g}^{-1}$ at 550 nm, a real RI value of 1.55, and a particle diameter of 200 nm were assumed, following the observations of Yang et al. (2009) and the study of Lack and Cappa (2010). The uncertainty in snow albedo considering the BC coating effect due to the OC MAC will be discussed in Sect. 3.4. Based on the Mie theory, an imaginary RI value of $-1.36 \times 10^{-2}i$ at 550 nm was calculated. Subse-

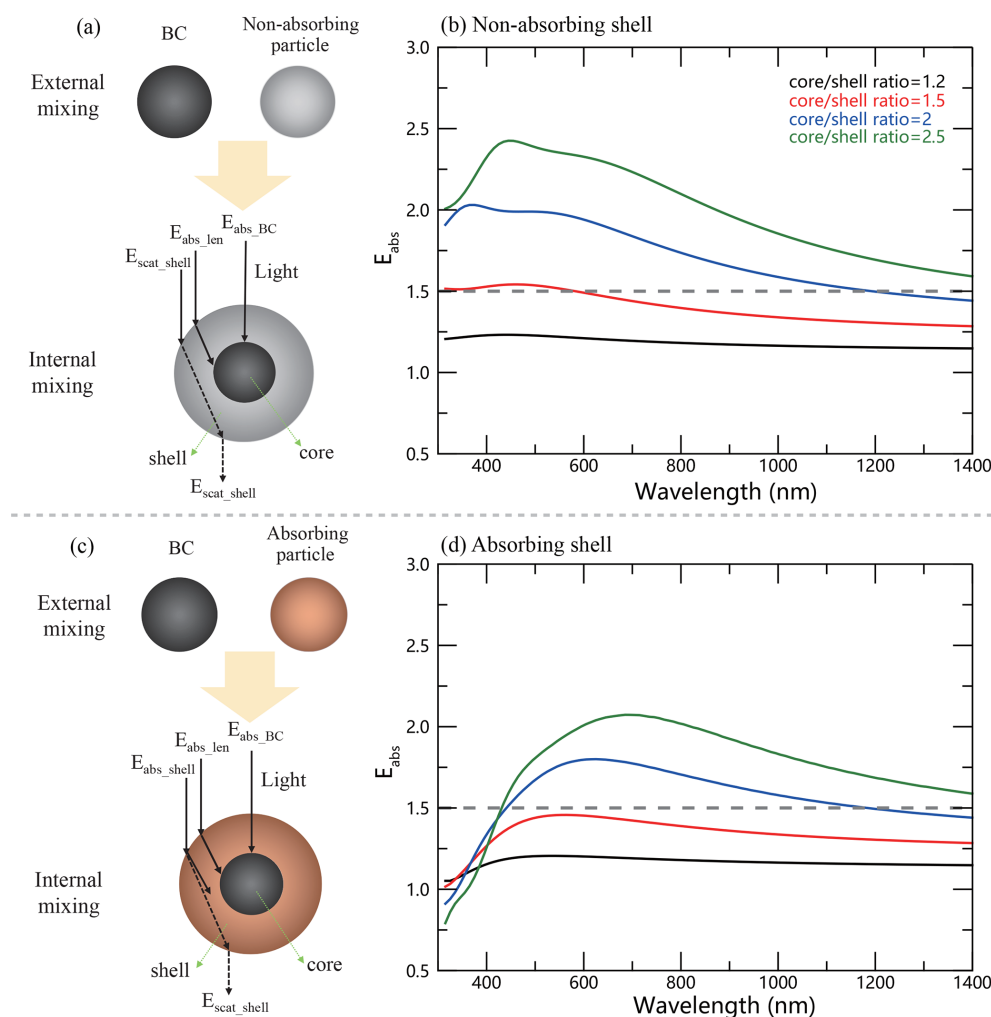


Figure 1. Schematic diagrams showing the light absorption of an external mixture and internal mixture of BC considering (a) a nonabsorbing particle and (c) an absorbing particle. Additionally, the enhancement of light absorption due to the internal mixture (E_{abs}) is compared to that due to the external mixture of BC with (b) nonabsorbing and (d) absorbing particles. The internal mixed particle was assumed to be a core / shell structure with a black carbon (BC) core.

quently, wavelength-dependent imaginary RI values (Fig. S1 in the Supplement) were derived according to an absorption Ångström exponent (AAE) of -6 (Sun et al., 2007).

In regard to a core / shell-structured particle, the core and shell diameters refer to the BC core diameter and the whole-particle diameter, respectively. The BC diameter usually ranges from ~ 50 – 120 nm in the atmosphere (Corbin et al., 2018) and is typically larger by ~ 20 nm in snow due to the removal process via wet deposition (Schwarz et al., 2013). Therefore, we assumed that the BC diameter in snow was 100 nm with a fixed monodisperse size distribution. The uncertainty in snow albedo of the BC coating effect due to the BC size distribution will be described in Sect. 3.4. The shell diameter was assumed to range from 110 to 300 nm based on Bond et al. (2006). The above core and shell diameters, RI, and wavelength were then applied in a Mie model to derive the optical parameters of core / shell particles, includ-

ing the single-scattering albedo (SSA), asymmetry factor (g), and extinction cross section (Q_{ext}). The mass extinction coefficient (MEC) of core / shell particles was calculated based on Q_{ext} and the density, given as 1.8 g cm^{-3} for BC (Bond et al., 2006), 1.2 g cm^{-3} for sulfate, and 1.2 g cm^{-3} for OC (Turpin and Lim, 2001).

2.1.2 Snow albedo calculations

We simulated snow albedo with the SNICAR model (Flanner et al., 2007), which calculates the radiative transfer in a snowpack based on the theory of Warren and Wiscombe (1980) and a two-stream multilayer radiative approximation (Toon et al., 1989). Here, we summarize only the model features in SNICAR that are crucial to our study. The SNICAR model allows for a vertical multilayer distribution of snow properties, LAPs, and heating throughout the snowpack col-

umn. The input optical parameters (MEC, SSA, and g) of snow grains and BC were calculated offline with the Mie theory. SNICAR provides snow albedo changes due to uncoated and sulfate-coated BC particles, in addition to dust particles and volcanic ash (for further details, please refer to Flanner et al., 2007).

In this study, we assumed a homogeneous semi-infinite snowpack and a solar zenith angle of 49.5° , whose cosine value (0.65) represents the insolation-weighted mean solar zenith cosine in the sunlit Earth hemisphere (Dang et al., 2015). The snow grain optical effective radius was varied from 50 to 1000 μm (at 50 μm intervals) to characterize snow aging. Moreover, the BC concentration was assumed to range from 0–1000 ng g^{-1} (at 10 ng g^{-1} intervals) to simulate clear to polluted snow, which was based on global field observations of the BC concentration in snowpacks mostly below 1000 ng g^{-1} (e.g., Doherty et al., 2010, 2014; Wang et al., 2013; Li et al., 2017, 2018; Pu et al., 2017; Zhang et al., 2017, 2018). These parameters were also applied in the subsequent parameterizations (please refer to Sect. 2.3). In addition, we note that the SNICAR model adopted in this study is the default version assuming BC–snow external mixing and spherical snow grains (Flanner et al., 2007). Although the mixing state of BC and snow grains and the snow grain shape affect the snow albedo, empirical parameterizations describing the effect of BC internally mixed with snow grains on snow albedo were developed by He et al. (2018c), and the albedo of a snowpack consisting of nonspherical snow grains was simulated with smaller spherical grains (Dang et al. 2016). Therefore, users may combine the empirical parameterizations developed by He et al. (2018c) and Dang et al. (2016) with our empirical parameterizations (please refer to Sect. 2.3) to study the effect of the internal mixing of BC with snow grains, snow grain shape, and coated BC particles on snow albedo.

Regarding the SNICAR snow albedo simulations considering uncoated BC particles, the concentrations of both BC and the other particles were directly input. Regarding coated BC particles, the optical parameters (MEC, SSA, and g) of IMPs (as calculated above) were first archived as lookup tables within the SNICAR model, and the IMP concentration was then input.

2.2 Calculation of the broadband snow albedo

The spectral albedo (α_λ) was integrated over the solar spectrum ($\lambda = 300\text{--}2500\text{ nm}$) and weighted based on the incoming solar irradiance (S_λ) to calculate the broadband snow albedo ($\alpha_{\text{integrated}}$):

$$\alpha_{\text{integrated}} = \frac{\int \alpha_\lambda S_\lambda d\lambda}{\int S_\lambda d\lambda}. \quad (1)$$

The considered incoming solar irradiance was the typical surface solar spectrum for midlatitudes–high latitudes from January to May, calculated with the Santa Barbara Discrete

Ordnate Radiative Transfer Atmospheric Radiative Transfer (SBDART) model (Pu et al., 2019), which is one of the most widely applied models in radiative transfer simulations (for further details, please refer to Ricchiazzi et al. 1998).

2.3 Parameterizations

In the original SNICAR model, the BC coating effect is simply parameterized with an absorption enhancement factor of ~ 1.5 (Flanner et al., 2007). However, the BC coating effect on snow albedo widely varies and depends on the BC concentration, core / shell ratio, snow grain size, and type of particle shell (please refer to Sect. 3.3). In view of this complexity, more explicit parameterizations were developed in this study:

$$E_{\alpha, \text{integrated}} = \frac{\alpha_{\text{int, integrated}}}{\alpha_{\text{ext, integrated}}}, \quad (2)$$

where $\alpha_{\text{ext, integrated}}$ and $\alpha_{\text{int, integrated}}$ are the broadband snow albedos for EMPs and IMPs, respectively. Following a previous empirical formulation (Hadley and Kirchstetter, 2012), $E_{\alpha, \text{integrated}}$ was parameterized as

$$E_{\alpha, \text{integrated, para}} = a_0 \times (C_{\text{BC}})^{a_1} + a_2, \quad (3)$$

$$a_1 = b_0 \times (\log_{10}(R_{\text{ef}}/50))^{b_1}, \quad (4)$$

where $E_{\alpha, \text{integrated, para}}$ is the parameterization of $E_{\alpha, \text{integrated}}$, C_{BC} is the BC concentration, and R_{ef} is the snow grain radius. The terms a_0 , a_1 , a_2 , b_0 , and b_1 are empirical coefficients that depend on the core / shell ratio and type of particle shell. To enhance the precision, the above parameterizations were divided into two groups: the first to consider relatively clean snow (at a BC concentration $< 200\text{ ng g}^{-1}$) and the second to consider relatively polluted snow ($200\text{ ng g}^{-1} < \text{BC concentration} < 1000\text{ ng g}^{-1}$).

2.4 Calculation of the in situ snow albedo and radiative forcing

In situ broadband clear-sky ($\alpha_{\text{integrated}}^{\text{clear, in situ}}$) and cloudy-sky ($\alpha_{\text{integrated}}^{\text{cloudy, in situ}}$) albedos were separately calculated based on corresponding in situ snow–LAP parameters and SBDART-simulated clear- and cloudy-sky incoming solar irradiance levels, respectively. We assumed a semi-infinite snowpack due to the limited available snow depth measurements. The BC and OC concentrations were collected from in situ field measurements (e.g., Doherty et al., 2010, 2014; Wang et al., 2013; Li et al., 2017, 2018; Pu et al., 2017; Zhang et al., 2017, 2018). A snow grain radius of 100 (1000) μm was assumed for fresh (old) snow, which is comparable to previous observations at midlatitude–high latitudes in winter (Wang et al., 2017; Shi et al., 2020). The value of the solar zenith angle was calculated based on the longitude, latitude, and sampling time at each sampling site. The in situ all-sky albedo ($\alpha_{\text{integrated}}^{\text{all-sky, in situ}}$) was then calculated based on weighted clear-

and cloudy-sky albedo values depending on the cloud fraction (CF), given as

$$\alpha_{\text{integrated}}^{\text{all-sky, in situ}} = \text{CF} \times \alpha_{\text{integrated}}^{\text{cloudy, in situ}} + (1 - \text{CF}) \times \alpha_{\text{integrated}}^{\text{clear, in situ}} \quad (5)$$

The in situ radiative forcing due to LAPs was calculated by multiplying the derived broadband albedo reduction by the downward shortwave flux at the snow surface (Dang et al., 2017). We note that the radiative forcing was calculated with the January–February average solar radiation in NA and NC and the April–May average solar radiation in the Arctic and Tibetan Plateau (TP) according to the periods of corresponding field campaigns. In this study, we mainly estimated the relative impacts of internal and external mixing on snow albedo and radiative forcing, which are hence not influenced by the chosen solar radiation level. Figure S2 in the Supplement shows spatial distributions of the solar flux and cloud fraction, which were obtained from the Clouds and the Earth’s Radiant Energy System (CERES) (<https://ceres.larc.nasa.gov/products.php?product=SYN1deg>, last access: 8 May 2021).

3 Results and discussion

3.1 Impact on particle light absorption

Figure 1b and d show the light absorption enhancement (E_{abs}) due to coated BC particles for the nonabsorbing and absorbing shells, respectively. E_{abs} is defined as the ratio of the light absorption due to coated (LA_{int}) and uncoated BC particles (LA_{ext}) ($E_{\text{abs}} = \text{LA}_{\text{int}}/\text{LA}_{\text{ext}}$). Based on Bond et al. (2006), we show the most common core / shell ratios (the ratio of the diameter of the whole particle to that of the BC core) of 1.2, 1.5, 2.0, and 2.5 in real environments to represent the thickness of shells, and we considered detailed core / shell ratios ranging from 1.1 to 3.0 (at intervals of 0.1) in the parameterizations (see Sect. 3.5). E_{abs} varies with the wavelength and increases with the core / shell ratio, in contrast to the default E_{abs} value employed in the original SNICAR model, which remains constant. Regarding nonabsorbing shells, the light absorption of IMPs is higher than that of EMPs across all wavelengths (300–1400 nm). Regarding absorbing shells, E_{abs} is similar to that of nonabsorbing shells in the NIR range but decreases in the visible (VIS) light and ultraviolet (UV) light ranges, which indicates that absorbing shells reduce whole-particle light absorption and negatively contribute to E_{abs} . This occurs because compared to the nonabsorbing shell, the absorbing shell, although it absorbs additional incident photons, causes fewer photons to reach the core, so that the photons absorbed by the lensing effect and BC core are reduced. In this case, the number of additional photons absorbed by the shell is smaller than the number of fewer photons absorbed by the lensing

effect and BC core, causing the total absorption of absorbing shell-coated BC particles to be lower than that of nonabsorbing shell-coated BC particles (Lack and Cappa, 2010). Furthermore, the absorbing shell reduces E_{abs} to < 1 in the UV range at high core / shell ratios, suggesting that the lensing effect on absorption at these wavelengths does not match the BC core absorption reduction, resulting in fewer photons reaching the core, which is similar to the results reported by Lack and Cappa (2010).

3.2 Impact on the spectral snow single-scattering properties and albedo

In a real snowpack, BC effectively enhances the snow single-scattering co-albedo ($1 - \omega$), but its effect on other snow optical parameters, such as the asymmetry factor and extinction efficiency, is negligible (He et al., 2017). Therefore, we focus our discussion on the coating-induced enhancement of the snow single-scattering co-albedo ($E_{1-\omega}$), snow albedo (E_{α}), and snow albedo reduction ($E_{\Delta\alpha}$). $E_{1-\omega}$ is defined as the ratio of the snow single-scattering co-albedo due to coated BC particles ($1 - \omega_{\text{int}}$) to that due to uncoated BC particles ($1 - \omega_{\text{ext}}$) ($E_{1-\omega} = (1 - \omega_{\text{int}})/(1 - \omega_{\text{ext}})$). Similar definitions were adopted for E_{α} ($E_{\alpha} = \alpha_{\text{int}}/\alpha_{\text{ext}}$) and $E_{\Delta\alpha}$ ($E_{\Delta\alpha} = (\Delta\alpha_{\text{int}})/(\Delta\alpha_{\text{ext}})$), where α_{int} and α_{ext} are the snow albedo values due to coated and uncoated BC particles, respectively, and $\Delta\alpha_{\text{int}}$ and $\Delta\alpha_{\text{ext}}$ are the snow albedo reductions due to coated and uncoated BC particles, respectively.

Figure 2 shows the variation in $1 - \omega$ and $E_{1-\omega}$ depending on the BC concentration, core / shell ratio, and coating material. Regarding either the nonabsorbing or absorbing shell, $1 - \omega_{\text{int}}$ is usually higher than $1 - \omega_{\text{ext}}$ in the VIS range, while the coating effect exerts little impact at wavelengths > 1200 nm because the optical properties of snow are mainly affected by LAPs in the VIS range but primarily by snow itself at wavelengths > 1200 nm. In addition, $E_{1-\omega}$ increases with increasing core / shell ratio, and the wavelength with the maximum $E_{1-\omega}$ value depends on the BC concentration and core / shell ratio. Moreover, the absorbing shell reveals a negative impact on $E_{1-\omega}$ over the nonabsorbing shell, especially in the UV range.

Snow albedo is notably influenced by various factors, such as the snow grain size, LAP content, and solar zenith angle, which has been widely examined and verified through model simulations and experimental measurements in previous studies (e.g., Warren and Wiscombe, 1980; Hadley and Kirchstetter, 2012; Wang et al., 2017). In this study, we mainly focus on the BC coating effect on snow albedo. Figure 3 shows the spectral snow albedo values due to coated (α_{int}) and uncoated BC particles (α_{ext}) and the ratios (E_{α}) of α_{int} to α_{ext} . Consistent with $1 - \omega$, the impact of the coating effect on snow albedo is mainly observed at wavelengths $< \sim 1200$ nm (Fig. 3a versus b and d versus e), where the higher the BC concentration (or the higher the core / shell ratio), the larger the difference in snow albedo between uncoated

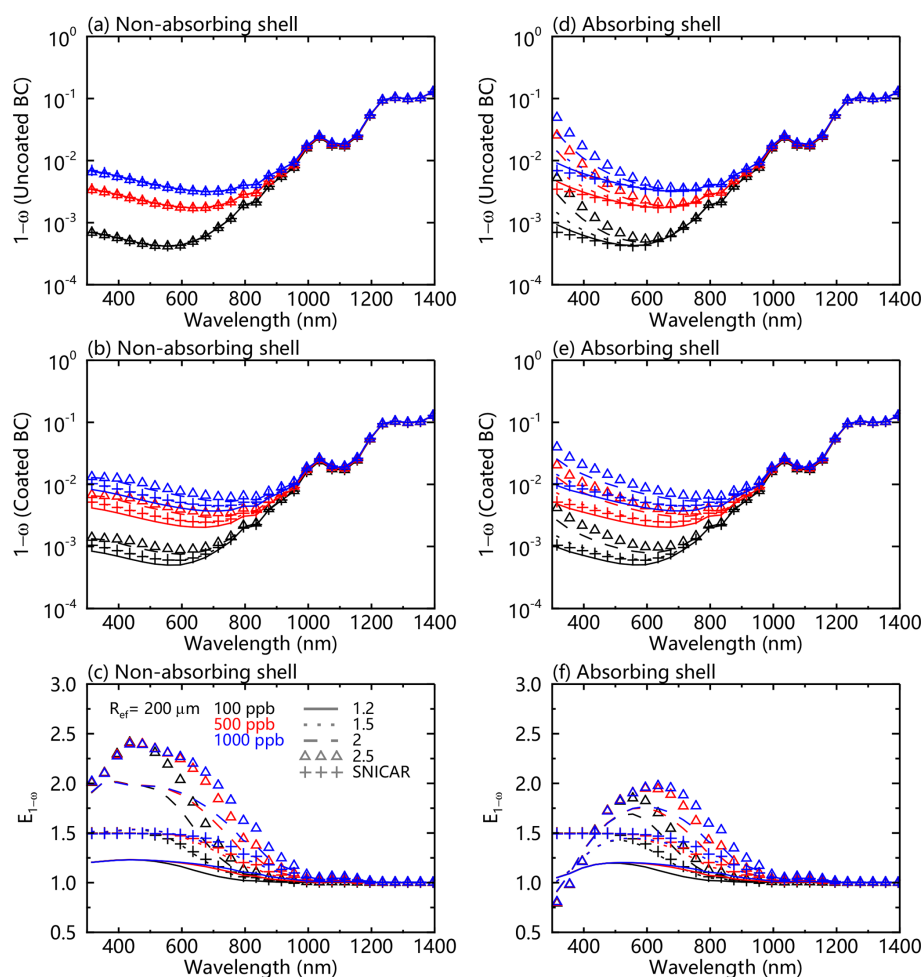


Figure 2. Snow single-scattering co-albedo ($1 - \omega$) as a function of the wavelength, at different BC concentrations and core / shell ratios for (a) uncoated and (b) coated BC particles under the assumption of a nonabsorbing shell. Panels (d) and (e) are the same as (a) and (b), respectively, but under the assumption of an absorbing shell. Panel (c) shows the ratios of the snow single-scattering co-albedo ($E_{1-\omega}$) for coated versus uncoated BC particles under the assumption of a nonabsorbing shell. Panel (f) is the same as (c) but under the assumption of an absorbing shell. The snow grain radius was assumed to be 200 nm.

and coated BC particles. Hadley and Kirchstetter (2012) also found a lower snow albedo due to internally mixed particles than that due to externally mixed particles. This phenomenon is also obvious for E_{α} , which decreases with increasing BC concentration and core / shell ratio in the VIS and NIR ranges (Fig. 3c and f, respectively). At a given BC concentration and core / shell ratio, E_{α} generally decreases with the wavelength from the UV range to the VIS range and then increases from the VIS range to the NIR range, which corresponds to the E_{abs} and $E_{1-\omega}$ results. In contrast, the E_{α} values considering the nonabsorbing and absorbing shells are comparable at wavelengths $> \sim 800$ nm. However, when the wavelength $< \sim 800$ nm, E_{α} considering the absorbing shell is higher than that considering the nonabsorbing shell, and the difference increases with decreasing wavelength and increasing core / shell ratio. Moreover, regarding the absorbing shells, the snow albedo due to coated BC particles is higher

than that due to uncoated BC particles at $< \sim 350$ nm at high core / shell ratios because the light absorption of internally mixed particles with absorbing shells is lower than that of externally mixed particles at the same wavelengths, as previously described in Sect. 3.1. These results indicate that the material of the particle shell also plays an important role in snow albedo in the UV and VIS ranges. We note that the solar radiative flux is very low at wavelengths < 350 nm, so that the coating effect at these wavelengths may contribute little to the total light absorption and broadband snow albedo but may potentially influence the photochemical reactions in a snowpack (Grannas et al., 2007).

Furthermore, Fig. 4 shows the spectral snow albedo reduction caused by coated ($\Delta\alpha_{\text{int}}$) and uncoated BC particles ($\Delta\alpha_{\text{ext}}$) and the ratio ($E_{\Delta\alpha}$) of $\Delta\alpha_{\text{int}}$ to $\Delta\alpha_{\text{ext}}$. Generally, $\Delta\alpha_{\text{int}}$ is larger than $\Delta\alpha_{\text{ext}}$, and the core / shell ratio dominates the variation in $E_{\Delta\alpha}$ across all wavelengths

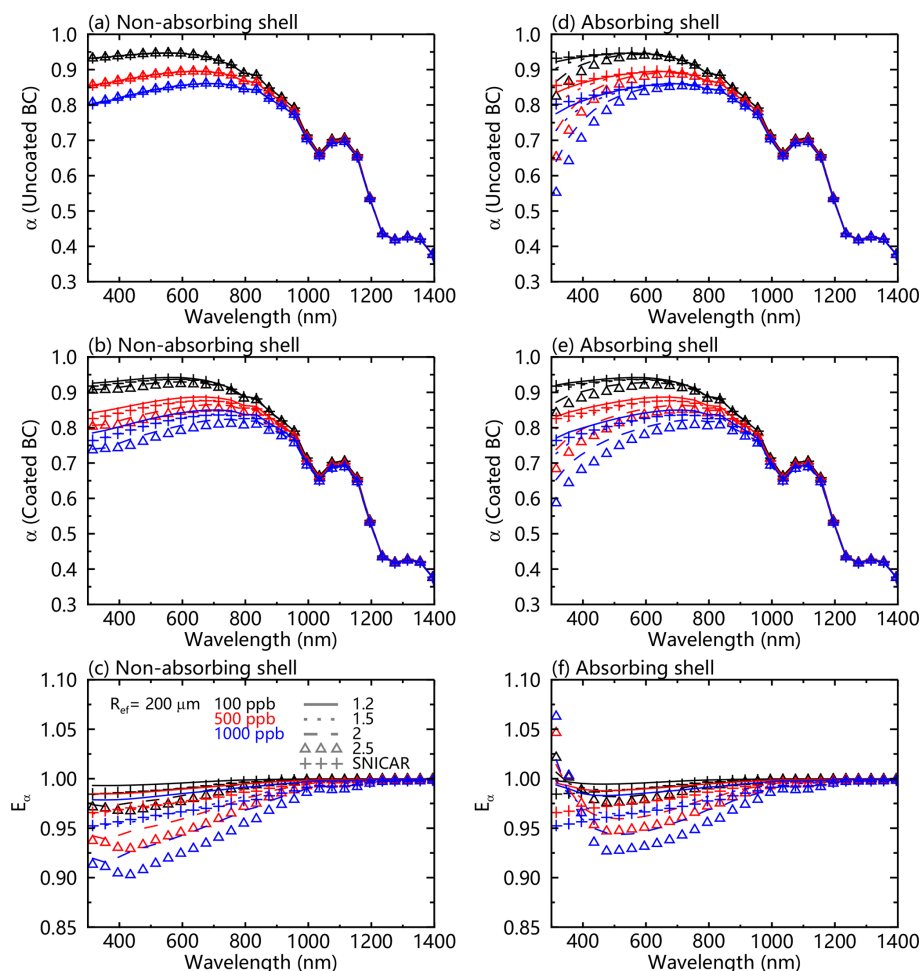


Figure 3. Same as Fig. 2, but for the snow albedo (α).

from 300–1400 nm, while the impact of the BC content is mainly manifested from 500–1000 nm. Consistent with $E_{1-\omega}$ and E_{α} , the impact of the material of the particle shell is negligible at a wavelength $> \sim 800$ nm, but $E_{\Delta\alpha}$ for the absorbing shell is lower than that for the nonabsorbing shell at a wavelength $< \sim 800$ nm. Moreover, $E_{\Delta\alpha}$ is < 1 for the absorbing shell at wavelengths $< \sim 350$ nm and high core/shell ratios. It is noteworthy that the coating effect still yields an obvious impact on snow albedo reduction at wavelengths $> \sim 1200$ nm, which is different from $E_{1-\omega}$ and E_{α} .

3.3 Impact on the broadband snow single-scattering properties and albedo

Compared to the spectral optical properties, our broadband results have wider implications for the research community. Figure 5 shows the spectrally weighted $1 - \omega$ due to coated ($1 - \omega_{\text{int,integrated}}$) and uncoated BC particles ($1 - \omega_{\text{ext,integrated}}$) and the ratio ($E_{1-\omega,\text{integrated}}$) of $1 - \omega_{\text{int,integrated}}$ to $1 - \omega_{\text{ext,integrated}}$. In general, $1 - \omega_{\text{int,integrated}}$ is larger than

$1 - \omega_{\text{ext,integrated}}$, and $E_{1-\omega,\text{integrated}}$ increases with the BC concentration and core/shell ratio but is little affected by the snow grain size. $E_{1-\omega,\text{integrated}}$ ranges from 1.0 to ~ 1.35 and 1.0 to ~ 1.23 for the nonabsorbing and absorbing shells, respectively, with the BC concentration lower than 1000 ng g^{-1} at core/shell ratios ranging from 1.2–2.5. At a given BC concentration and core/shell ratio, $E_{1-\omega,\text{integrated}}$ considering the nonabsorbing shell is higher than that considering the absorbing shell. In addition, $E_{1-\omega,\text{integrated}}$ determined with the original SNICAR model is close to that considering the nonabsorbing shell at a core/shell ratio of 1.5.

Figure 6 shows the spectrally weighted snow albedo due to coated ($\alpha_{\text{int,integrated}}$) and uncoated BC particles ($\alpha_{\text{ext,integrated}}$) and the ratio ($E_{\alpha,\text{integrated}}$) of $\alpha_{\text{int,integrated}}$ to $\alpha_{\text{ext,integrated}}$. Generally, $\alpha_{\text{int,integrated}}$ is lower than $\alpha_{\text{ext,integrated}}$ by 0 to 0.069 (0 to 0.051), and $E_{\alpha,\text{integrated}}$ ranges from 1 to ~ 0.903 (1 to ~ 0.924) considering the nonabsorbing (absorbing) shell at BC concentrations from 0 to 1000 ng g^{-1} , with the snow grain radius ranging from 100 to $500 \mu\text{m}$ and the core/shell ratio ranging from 1.2 to 2.5. $E_{\alpha,\text{integrated}}$ exhibits a decreasing trend with increasing BC

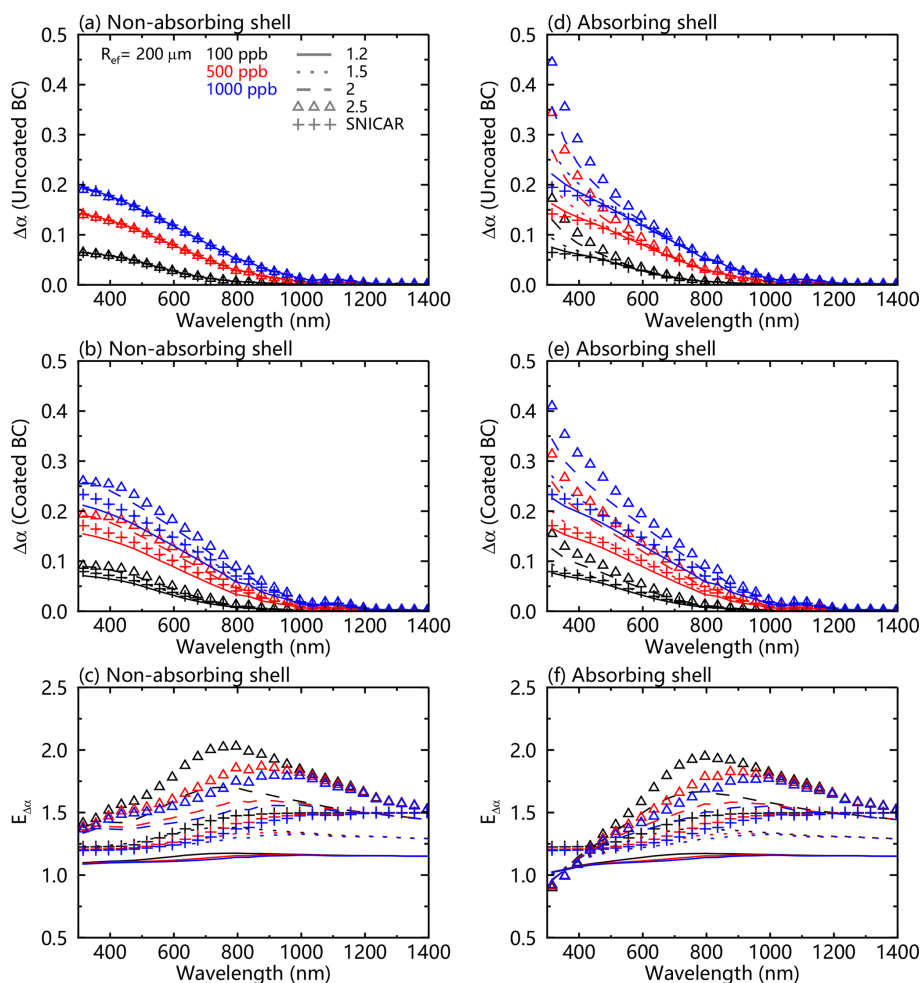


Figure 4. Same as Fig. 2, but for the snow albedo reduction ($\Delta\alpha$).

concentration, core / shell ratio, and snow grain size. In addition, the difference between $\alpha_{\text{ext,integrated}}$ and $\alpha_{\text{int,integrated}}$ (or $E_{\alpha,\text{integrated}}$) for the nonabsorbing shell is larger (or smaller) than that for the absorbing shell. If considering these coating effects in real environments, e.g., in clean snow, such as in North America at a typical BC concentration of $\sim 50 \text{ ng g}^{-1}$ (Doherty et al., 2014), the difference between $\alpha_{\text{ext,integrated}}$ and $\alpha_{\text{int,integrated}}$ ranges from 0.002–0.017 and 0.001–0.012 considering the nonabsorbing and absorbing shells, respectively, at core / shell ratios from 1.2–2.5 and snow grain radii from 100–500 μm . In contrast, in polluted snow, such as in northeastern China, the BC concentration is typically $\sim 1000 \text{ ng g}^{-1}$ in industrial regions. The difference between $\alpha_{\text{ext,integrated}}$ and $\alpha_{\text{int,integrated}}$ ranges from 0.008–0.069 and 0.007–0.051 considering the nonabsorbing and absorbing shells, respectively. These results indicate that the impact of the coating effect on snow albedo may lead to a reduction in snow albedo by $\sim 2\%$ in clean snow and $\sim 10\%$ in polluted snow due to coated BC particles below the snow albedo due to uncoated BC particles. In addition, the sensitivity of

$E_{\alpha,\text{integrated}}$ to BC decreases with increasing BC concentration due to the nonlinear effect of BC on snow albedo (Flanner et al., 2007).

Figure 7 shows the spectrally weighted snow albedo reduction due to coated ($\Delta\alpha_{\text{int,integrated}}$) and uncoated BC particles ($\Delta\alpha_{\text{ext,integrated}}$) and the ratio ($E_{\Delta\alpha,\text{integrated}}$) of $\Delta\alpha_{\text{int,integrated}}$ to $\Delta\alpha_{\text{ext,integrated}}$. In contrast to $E_{\alpha,\text{integrated}}$, $E_{\Delta\alpha,\text{integrated}}$ is dominated by the core / shell ratio but slightly depends on the snow grain size (Figs. 7c and 6f, respectively). In addition, $E_{\Delta\alpha,\text{integrated}}$ exhibits a slight decreasing trend with increasing BC concentration. Comparing Fig. 7c and f, we find that the particle shell material exerts a distinct integrated impact on $E_{\Delta\alpha}$. $E_{\Delta\alpha,\text{integrated}}$ mostly ranges from 1.11 to ~ 1.80 (1.10 to ~ 1.33) for the nonabsorbing (absorbing) shells at core / shell ratios from 1.2 to 2.5. Our results are comparable to those of a previous study in which the snow albedo reduction due to BC–snow internal mixing was larger than that due to external mixing by a factor of 0.2–1.0 (He et al., 2018c). However, the $E_{\Delta\alpha,\text{integrated}}$ value retrieved from the original SNICAR model demon-

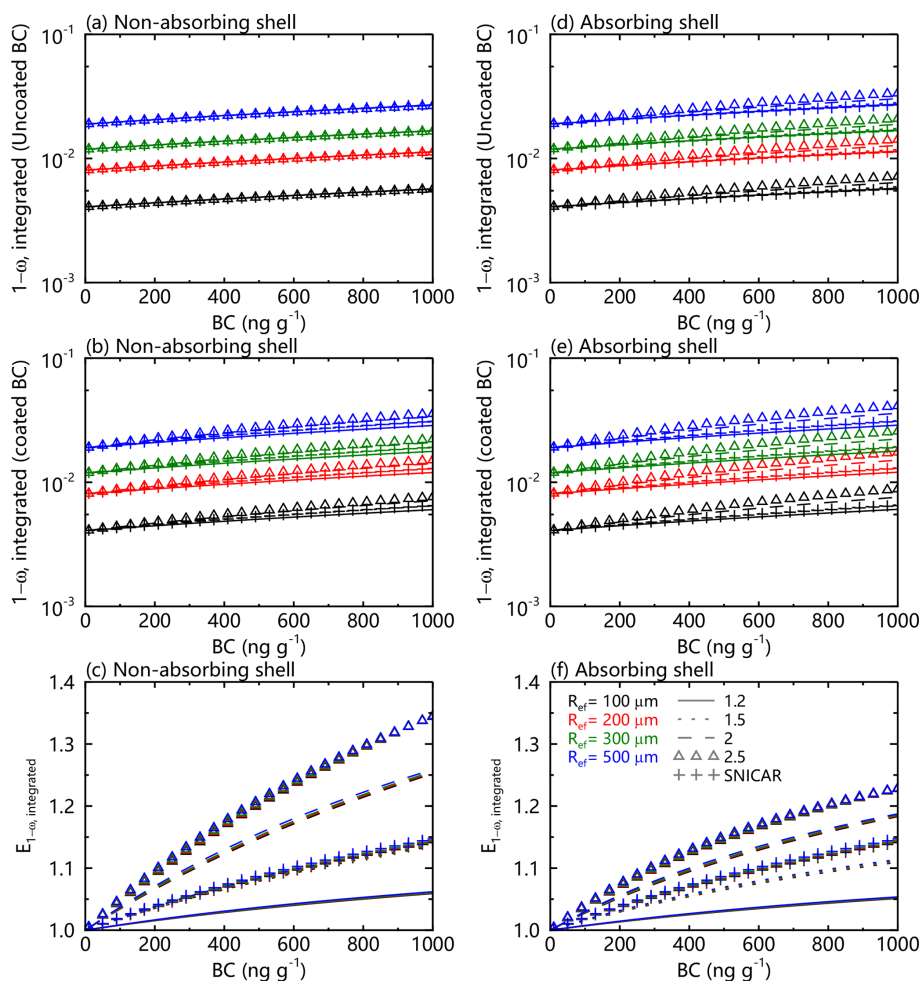


Figure 5. Spectrally weighted snow single-scattering co-albedo ($1 - \omega_{\text{integrated}}$) from 300–2500 nm of the typical surface solar spectrum at midlatitudes–high latitudes from January to May for (a) uncoated and (b) coated BC particles under the assumption of a nonabsorbing shell. Panels (d) and (e) are the same as (a) and (b), respectively, but under the assumption of an absorbing shell. Panel (c) shows the ratios ($E_{1-\omega, \text{integrated}}$) of the spectrally weighted snow single-scattering co-albedo for coated versus uncoated BC particles under the assumption of a nonabsorbing shell. Panel (f) is the same as (c) but under the assumption of an absorbing shell.

strates only a small variation from 1.23–1.31. This is similar to the nonabsorbing shell at a core / shell ratio of ~ 1.5 , which suggests that the original SNICAR model only reflects the coating effect on snow albedo reduction at an intermediate core / shell ratio, which may lead to possible biases ranging from -10% to 50% in snow albedo reduction calculations.

3.4 Uncertainties

Although the imaginary RI value of OC has been theoretically calculated (Sect. 2.1), we note that in a real snowpack, there exists a high uncertainty because the types and optical properties of OC vary spatially and temporally due to different emission sources and photochemical reactions in the atmosphere (e.g., Lack and Cappa, 2010). To address this issue, we tested the degree of influence of the imaginary RI

value on the $E_{\alpha, \text{integrated}}$ and $E_{\Delta\alpha, \text{integrated}}$ values by increasing and decreasing the calculated imaginary RI value by 50% (Fig. S1), which studies have revealed to be plausible (e.g., Lack et al., 2012). We found the imaginary RI uncertainty to be $\pm 1\%$ for $E_{\alpha, \text{integrated}}$ and $\pm 5\%$ for $E_{\Delta\alpha, \text{integrated}}$.

In addition, observations have demonstrated large variations in the size distribution of atmospheric and snowpack BC particles (Schwarz et al., 2013), which may affect the snow optical properties and albedo (He et al., 2018b). Therefore, we examined the effects of the BC particle size on $E_{\alpha, \text{integrated}}$ and $E_{\Delta\alpha, \text{integrated}}$ with two additional BC particle diameters of 50 and 150 nm, which occur within the observed size ranges (Schwarz et al., 2013) and are comparable to the BC particle sizes adopted in other studies (e.g., He et al., 2018b). We find that the uncertainty attributed to the BC particle diameter is $\pm 1\%$ for $E_{\alpha, \text{integrated}}$ and $\pm 13\%$ for $E_{\Delta\alpha, \text{integrated}}$. According to Eq. (2), the uncertainty in

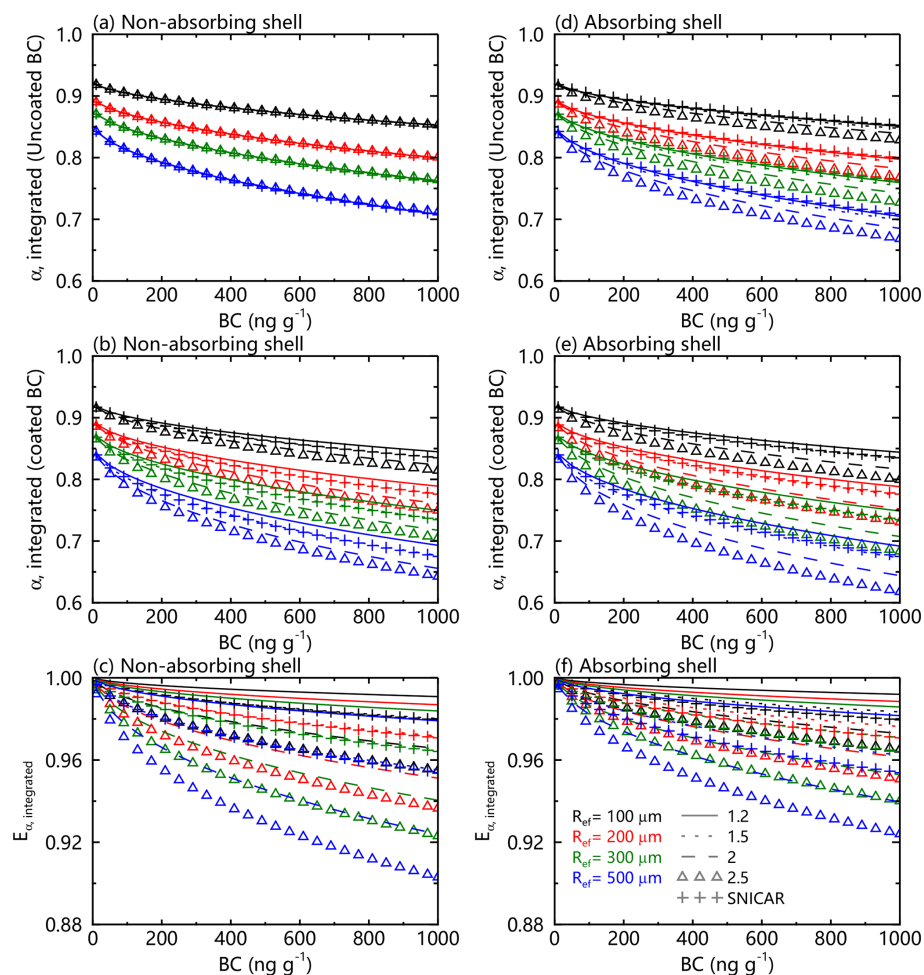


Figure 6. Same as Fig. 5, but for the snow albedo ($\alpha_{\text{integrated}}$).

$E_{\alpha, \text{integrated}}$ is equivalent to that in the snow albedo, and the uncertainty in $E_{\Delta\alpha, \text{integrated}}$ is equivalent to that in the snow albedo reduction. Therefore, the total uncertainty related to the imaginary RI value, and BC particle diameter is $\pm 1.4\%$ for $E_{\alpha, \text{integrated}}$ (snow albedo) and $\pm 13.9\%$ for $E_{\Delta\alpha, \text{integrated}}$ (snow albedo reduction).

Another important issue is that in real environments, BC mixtures containing other species are likely much more complex than uniform coatings on spheres. Hence, a core / shell assumption seems somewhat dubious. However, a recent study observing the individual particle structure and mixing states between glaciers–snowpacks and the atmosphere (Dong et al., 2018) has found that fresh BC particles are generally characterized by a fractal morphology, which abundantly occurs in the atmosphere. In contrast, in a snowpack, aged BC particles dominated the BC content, and the mixing states of aged BC particles largely changed to internal mixing forms with BC at the core. This process was characterized by the initial transformation from a fractal structure to a spherical morphology and the subsequent growth of fully

compact particles during the transport and deposition process. Therefore, a core / shell assumption for coated BC particles in a snowpack seems to be plausible. In addition, most field measurements have not captured the explicit structure of coated BC particles due to the limited observation methods (e.g., Doherty et al., 2010, 2014; Wang et al., 2013; Li et al., 2017, 2018; Pu et al., 2017; Zhang et al., 2017, 2018); therefore, even if a model of the explicit BC structure was developed, researchers experience difficulties studying the effect of coated BC particles on snow albedo reduction at present. Moreover, a core / shell assumption for coated BC particles in the atmosphere has been widely applied in most global climate models (e.g., Jacobson, 2001; Bond et al. 2013), so our parameterizations describing coated BC particles in a snowpack may be easily linked to these models. In summary, we indicate that a core / shell assumption describing coated BC particles in a snowpack is plausible and practical for field observations and model simulations at present despite possible uncertainties. However, with the development of measurement methods and climate models, a more explicit structure

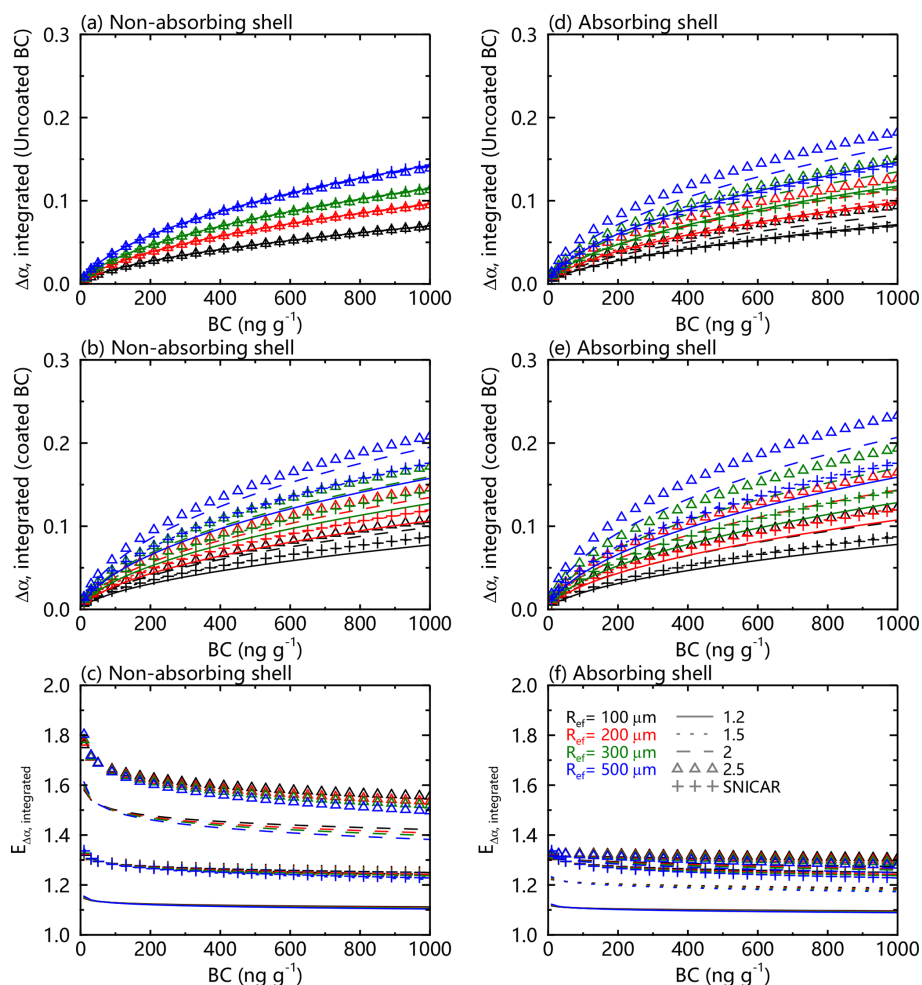


Figure 7. Same as Fig. 5, but for the snow albedo reduction ($\Delta\alpha_{\text{integrated}}$).

characterizing coated BC particles in a snowpack is actually needed in the future.

3.5 Parameterizations of the coating effect

Figure 8 compares parameterized $E_{\alpha,\text{integrated,para}}$ values to SNICAR-modeled $E_{\alpha,\text{integrated}}$ values, and Tables S1 and S2 in the Supplement, respectively, list the empirical coefficients (please refer to Sect. 2.3) derived from the nonlinear regression process. This parameterization is applicable under the assumptions of a semi-infinite snowpack, BC–snow external mixing, and spherical snow grains, as mentioned in Sect. 2. Generally, $E_{\alpha,\text{integrated,para}}$ and $E_{\alpha,\text{integrated}}$ exhibit a strong correlation, with $R^2 = 0.988$ (0.986) for the nonabsorbing shell and $R^2 = 0.987$ (0.986) for the absorbing shell in relatively clean (polluted) snow and root-mean-squared errors of 1.81×10^{-3} (4.70×10^{-3}) and 1.41×10^{-3} (3.76×10^{-3}), respectively. The biases in $E_{\alpha,\text{integrated,para}}$ are the lowest at intermediate BC concentrations but become relatively high at extremely low or high concentrations, mainly due to processes within the nonlinear regression method. In addition,

the snow grain size exerts a limited impact on the accuracy of the parameterized results so that these parameterizations can be applied to either fresh or old snow types. Overall, the integrated E_{α} value is suitably reproduced by $E_{\alpha,\text{integrated,para}}$, and the parameterizations are applicable under various snow pollution conditions at BC concentrations ranging from 0–1000 ng g^{-1} , core / shell ratios ranging from 1.1 to 3.0, and different coating materials (nonabsorbing and absorbing shells). We note that if the BC concentration is higher than 1000 ng g^{-1} , the parameterization describing relatively polluted snow is also applicable with a low negative bias.

Therefore, future studies may estimate the BC coating effect on snow albedo and radiative forcing very conveniently by combining the original SNICAR model or other snow radiative forcing models with our new parameterizations, which may reduce the snow albedo simulation bias. However, although most global climate models (GCMs) account for coated BC particles in the atmosphere, they barely consider the BC coating effect in snow (Bond et al., 2013). In

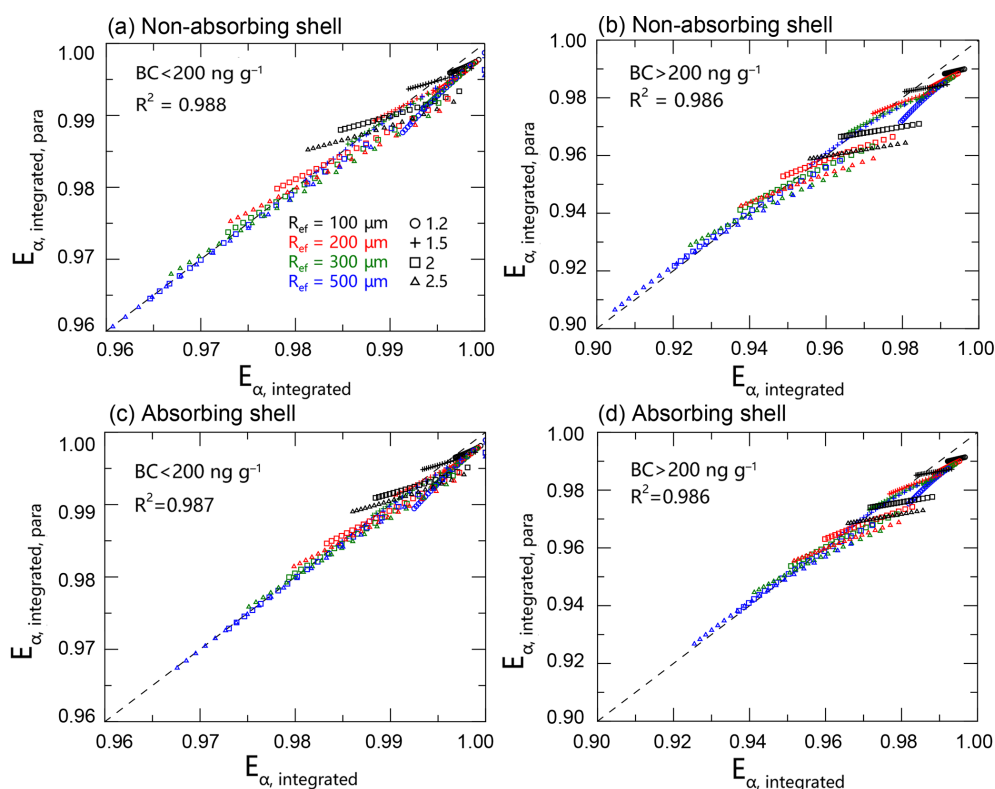


Figure 8. Comparisons of model-calculated $E_{\alpha, \text{integrated}}$ and parameterized $E_{\alpha, \text{integrated, para}}$ values for (a) relatively clean snow (BC concentration $< 200 \text{ ng g}^{-1}$) and (b) relatively polluted snow (BC concentration $> 200 \text{ ng g}^{-1}$) for a nonabsorbing shell. Panels (c) and (d) are the same as (a) and (b), respectively, but for an absorbing shell.

addition, different GCMs apply varying types of snow radiative transfer models, which indicates that one physical mechanism describing the BC coating effect in snow may not be suitable for all GCMs. Hence, our parameterizations are suitable for climate models and provide an option to capture BC coating effects in snow.

3.6 Measurement-based estimate of the coating effect

To evaluate the BC coating effect on both the snow albedo and radiative forcing in a real snowpack, we collected in situ measurements of BC and OC concentrations in snow (Fig. 9) during field campaigns in the Arctic in the spring from 2007–2009 (Doherty et al., 2010), in North America from January–March 2013 (Doherty et al., 2014), in northern China from January–February 2010 and 2012 (Ye et al., 2012; Wang et al., 2013), and on the Tibetan Plateau in the spring of 2010 and 2012 (Wang et al., 2013; Li et al., 2017, 2018; Pu et al., 2017; Zhang et al., 2017, 2018). The measurements were separated into four geographical regions (Fig. 9c): the Arctic, North America (NA), northern China (NC), and the Tibetan Plateau (TP). An absorbing shell consisting of OC was assumed in the measured snowpack data, which is plausible because previous studies have found that OC is the dominant coating in the atmosphere (e.g., Cappa et al., 2012) and snow

(Dong et al., 2018). The OC/BC mass ratio generally ranges from 1 to 10, with the corresponding core / shell ratio ranging from 1.3 to 2.5 (Fig. 9b). The average core / shell ratio was the highest (2.45) on the TP, followed by values of 1.92 and 1.81 in the Arctic and NC, respectively, and was the lowest (1.31) in NA (Fig. 9d). These results reveal that the BC coating effect exerted a larger impact on snow albedo on the TP than that in the other regions. In this study, the assumption that all measured OC occurs as a coating on BC particles was mainly adopted to reveal the upper bound of the coating effect on snow albedo reduction, which is comparable to previous studies (e.g., He et al. 2018c).

Figure 10 shows statistics of the snow albedo reduction and radiative forcing in the different regions for fresh snow (snow grain radius = $100 \mu\text{m}$) and old snow (snow grain radius = $1000 \mu\text{m}$). Spatial distributions of the attained snow albedo reduction and radiative forcing are shown in Figs. S3 and S4 in the Supplement, respectively. Briefly, the TP snowpack suffers the highest snow albedo reduction (0.066), and the regional average snow albedo reduction is lower in NC (0.055), NA (0.009), and the Arctic (0.007) for fresh snow in the case of external mixing (Fig. 10a). Accordingly, the regional average radiative forcing is 11.63, 4.42, 0.97, and 0.56 W m^{-2} on the TP, NC, NA, and the Arctic, respec-

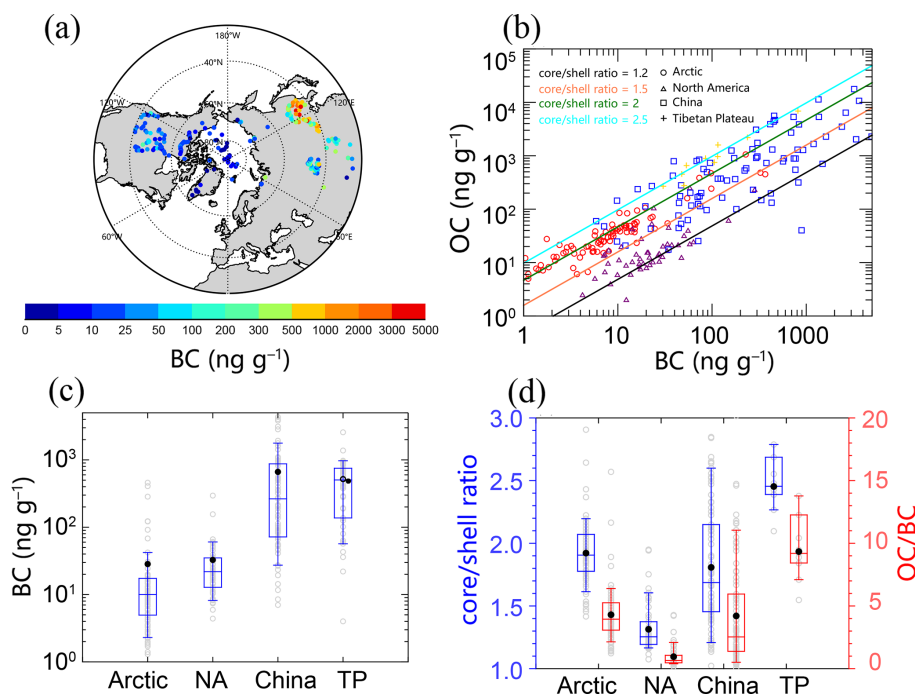


Figure 9. (a) Spatial distribution of the measured black carbon (BC) concentration across the Northern Hemisphere. (b) Comparison of the BC and organic carbon (OC) concentrations in the Arctic, North America (NA), northern China (NC), and the Tibetan Plateau (TP). (c) Statistical plots of the BC concentration in the different regions. The boxes denote the 25th and 75th quantiles, the horizontal lines denote the 50th quantiles (median values), the solid dots denote the average values, and the whiskers denote the 10th and 90th quantiles. The in situ data are shown as gray circles. Panel (d) is the same as (c) but for the core / shell ratio and OC/BC mass ratio, assuming a core / shell structure with a BC core and an absorbing OC shell.

tively (Fig. 10b). In the case of internal mixing, the regional average snow albedo reduction is 0.084, 0.065, 0.011, and 0.009 on the TP, NC, NA, and the Arctic, respectively, with corresponding radiative forcings of 14.84, 5.51, 1.11, and 0.69 W m^{-2} , respectively. Figure 11 shows a comparison of internal mixing to external mixing. In fresh snow, we find that coated BC particles result in greater snow albedo reductions than those due to uncoated BC particles by factors of 1.27, 1.19, 1.13, and 1.23 on the TP, NC, NA, and the Arctic, respectively (Fig. 11a and b, respectively). Correspondingly, we find that the coating effect yields radiative forcing enhancements of 1.27, 1.20, 1.14, and 1.22, respectively, in these regions. The largest (smallest) enhancement was found on the TP (NA), which corresponds to the highest (lowest) OC/BC mass ratio and core / shell ratio on the TP (NA). In regard to old snow, the regional average snow albedo reduction is 0.17 (0.21), 0.14 (0.17), 0.028 (0.033), and 0.022 (0.027) on the TP, NC, NA, and the Arctic, respectively, for external (internal) mixing (Fig. 10c). The corresponding radiative forcings are 38.2 (47.6), 19.2 (22.7), 4.6 (5.2), and $3.6 (4.6) \text{ W m}^{-2}$, respectively (Fig. 10d). The enhancement of snow albedo reduction due to the BC coating effect is 1.24, 1.15, 1.13, and 1.23 on the TP, NC, NA, and the Arctic, respectively (Fig. 11c). The corresponding enhancement of radiative forcing is 1.24, 1.16, 1.14, and 1.22, respectively

(Fig. 11d). The enhancement exhibits a slight decrease with snowpack aging, which is consistent with the results shown in Fig. 7. Notably, we found that the contribution of the coating effect to light absorption exceeded that of dust over most areas of northern China after comparison to previous studies of dust in snow (Wang et al., 2013, 2017; Pu et al., 2017), which further demonstrated the critical role of the BC coating effect in snow albedo evaluation.

In contrast to previous studies, we note that an enhanced light absorption in snow due to the BC coating effect should be considered, especially in the Arctic and TP. Arctic sea ice has sharply declined in recent decades (Ding et al., 2019), and climate models predict a continued decreasing trend (Liu et al., 2020) that is likely to perturb the Earth system and influence human activities (Meier et al., 2014). Multimodel ensemble simulations have indicated that greenhouse gases cannot fully explain this decline, and recent studies have proposed that BC deposition in snow and sea ice is an important additional contributor (e.g., Ramanathan and Carmichael, 2008). Furthermore, the TP holds the largest ice mass outside the polar regions and acts as a water storage tower for more than 1 billion people in South and East Asia. Tibetan glaciers have rapidly retreated over the last 30 years (Yao et al., 2012), raising the possibility that many glaciers and their freshwater supplies could disappear by the middle of

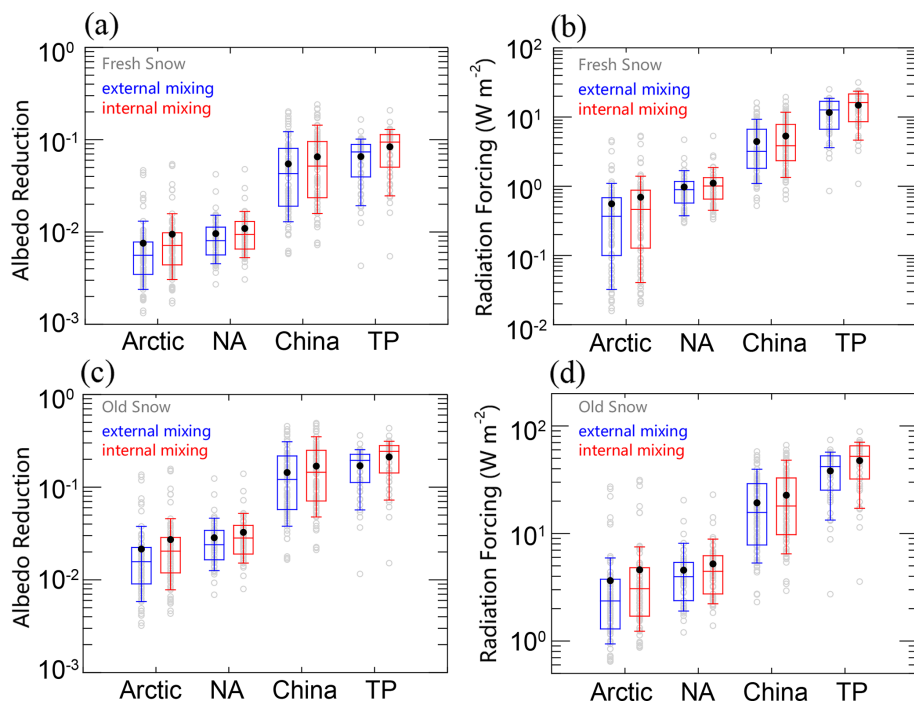


Figure 10. Statistical plots of (a) albedo reduction and (b) radiative forcing in the different regions for fresh snow. Panels (c) and (d) are the same as (a) and (b), respectively, but for old snow. The boxes denote the 25th and 75th quantiles, the horizontal lines denote the 50th quantiles (median values), the solid dots denote the average values, and the whiskers denote the 10th and 90th quantiles. The in situ data are shown as gray circles.

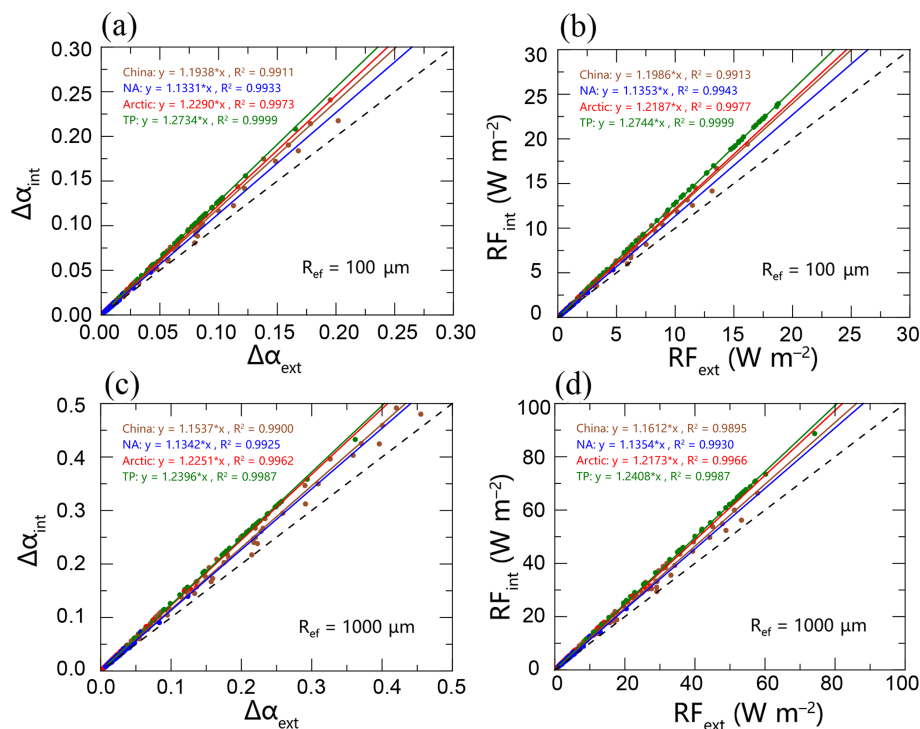


Figure 11. Comparisons of (a) snow albedo reduction and (b) radiative forcing via internally mixed particles versus externally mixed particles based on in situ measurements of fresh snow (assuming a snow grain radius of $100 \mu\text{m}$). Panels (c) and (d) are the same as (a) and (b), respectively, but for old snow and assuming a snow grain radius of $1000 \mu\text{m}$.

the 21st century. Observed evidence has suggested that BC deposition is a major contributing factor to this retreat (Xu et al., 2009), but the quantitative modeling of the BC effect on glacier dynamics is a challenge, partly because of the incomplete radiative transfer mechanisms within current models. Due to the notable contribution of BC to the retreat in Arctic sea ice and Tibetan glaciers and the strong enhancement of light absorption due to coated BC particles, the coating effect must now be considered in climate models that are designed to accurately reconstruct both historical records and future changes.

4 Conclusions

This study evaluated the BC coating effect on snow albedo and radiative forcing by combining the core/shell Mie theory and snow albedo SNICAR model. We found that the coating effect enhances snow albedo reduction by a factor of 1.11–1.80 for the nonabsorbing shell and 1.10–1.33 for the absorbing shell at BC concentrations below 1000 ng g^{-1} , a snow grain radius ranging from 100–500 μm , and a core/shell ratio ranging from 1.2–2.5. The core/shell ratio plays a dominant role in snow albedo reduction. Furthermore, the absorbing shell causes a smaller snow albedo reduction than that caused by the nonabsorbing shell because of the lensing effect, whereby the absorbing shell reduces photon absorbance in the BC core. Our results effectively considered the complex enhancement of snow albedo reduction due to the coating effect in real environments.

Parameterizations describing the coating effect were further developed for application in snow albedo and climate models. The parameterized and simulated results exhibit strong correlations in both clean and polluted snowpacks. The root-mean-squared error of the parameterized $E_{\alpha, \text{integrated, para}}$ values is small (1.41×10^{-3}). A list of empirical coefficients for parameterizations was provided suitable for most seasonal snowpack field cases, with BC concentrations lower than 1000 ng g^{-1} , snow grain sizes ranging from 50–1000 μm , and core/shell ratios ranging from 1.1 to 3.0. We demonstrated that these parameterizations could reduce the simulation bias regarding local experiments in snow albedo models and, more importantly, could be applied to GCMs to improve our understanding of how BC in snow affects local hydrological cycles and the global climate.

Based on a comprehensive set of field measurements across the Northern Hemisphere, the BC coating effect in real snowpacks was evaluated by assuming the presence of an absorbing OC shell. The enhancement of snow albedo reduction ranged from 1.13–1.27, and the enhancement of radiative forcing was 1.14–1.27, which exceeds the contribution of dust to snow light absorption over most areas of northern China. Notably, the greatest enhancements were detected on the Tibetan Plateau and in the Arctic, which may likely contribute to further Arctic sea ice and Tibetan glacier retreat.

Our findings indicated that the coating effect must be considered in future climate models, in particular to evaluate the climate on the Tibetan Plateau and Arctic more accurately.

Code and data availability. All codes and data sets used to produce this study can be obtained by contacting Xin Wang (wxin@lzu.edu.cn).

Supplement. The supplement related to this article is available online at: <https://doi.org/10.5194/tc-15-2255-2021-supplement>.

Author contributions. XW and WP invited the project. WP and XW designed the study. WP wrote the paper with contributions from all co-authors. TLS processed and analyzed the data.

Competing interests. The authors declare that they have no conflict of interest.

Acknowledgements. We are grateful for the constructive comments and suggestions from the editor Mark Flanner and the two anonymous referees.

Financial support. This research has been supported by the National Science Fund for Distinguished Young Scholars (42025102), the National Key Research and Development Program of China (grant number 2019YFA0606801), the National Natural Science Foundation of China (grant numbers 42075061, 41975157, and 41775144), and the China Postdoctoral Science Foundation (2020M673530).

Review statement. This paper was edited by Mark Flanner and reviewed by two anonymous referees.

References

- Aquila, V., Hendricks, J., Lauer, A., Riemer, N., Vogel, H., Baumgardner, D., Minikin, A., Petzold, A., Schwarz, J. P., Spackman, J. R., Weinzierl, B., Righi, M., and Dall'Amico, M.: MADE-in: a new aerosol microphysics submodel for global simulation of insoluble particles and their mixing state, *Geosci. Model Dev.*, 4, 325–355, <https://doi.org/10.5194/gmd-4-325-2011>, 2011.
- Bond, T. C., Habib, G., and Bergstrom, R. W.: Limitations in the enhancement of visible light absorption due to mixing state, *J. Geophys. Res.-Atmos.*, 111, D20211, <https://doi.org/10.1029/2006JD007315>, 2006.
- Bond, T. C., Doherty, S. J., Fahey, D. W., Forster, P. M., Berntsen, T., DeAngelo, B. J., Flanner, M. G., Ghan, S., Karcher, B., Koch, D., Kinne, S., Kondo, Y., Quinn, P. K., Sarofim, M. C., Schultz, M. G., Schulz, M., Venkataraman, C., Zhang, H., Zhang, S., Bellouin, N., Guttikunda, S. K., Hopke, P. K., Jacobson, M. Z.,

- Kaiser, J. W., Klimont, Z., Lohmann, U., Schwarz, J. P., Shindell, D., Storelvmo, T., Warren, S. G., and Zender, C. S.: Bounding the role of black carbon in the climate system: A scientific assessment, *J. Geophys. Res.-Atmos.*, 118, 5380–5552, 2013.
- Cappa, C. D., Onasch, T. B., Massoli, P., Worsnop, D. R., Bates, T. S., Cross, E. S., Davidovits, P., Hakala, J., Hayden, K. L., Jobson, B. T., Kolesar, K. R., Lack, D. A., Lerner, B. M., Li, S. M., Mellon, D., Nuaaman, I., Olfert, J. S., Petaja, T., Quinn, P. K., Song, C., Subramanian, R., Williams, E. J., and Zaveri, R. A.: Radiative Absorption Enhancements Due to the Mixing State of Atmospheric Black Carbon, *Science*, 337, 1078–1081, 2012.
- Cohen, J. and Rind, D.: The effect of snow cover on the climate, *J. Climate*, 4, 689–706, 1991.
- Corbin, J. C., Pieber, S. M., Czech, H., Zanatta, M., Jakobi, G., Massabò, D., Orasche, J., El Haddad, I., Mensah, A. A., and Stengel, B.: Brown and black carbon emitted by a marine engine operated on heavy fuel oil and distillate fuels: optical properties, size distributions, and emission factors, *J. Geophys. Res.-Atmos.*, 123, 6175–6195, 2018.
- Dang, C., Brandt, R. E., and Warren, S. G.: Parameterizations for narrowband and broadband albedo of pure snow and snow containing mineral dust and black carbon, *J. Geophys. Res.-Atmos.*, 120, 5446–5468, 2015.
- Dang, C., Fu, Q., and Warren, S. G.: Effect of Snow Grain Shape on Snow Albedo, *J. Atmos. Sci.*, 73, 3573–3583, 2016.
- Dang, C., Warren, S. G., Fu, Q., Doherty, S. J., and Sturm, M.: Measurements of light-absorbing particles in snow across the Arctic, North America, and China: effects on surface albedo, *J. Geophys. Res.-Atmos.*, 122, 10149–10168, 2017.
- Ding, Q., Schweiger, A., L'Heureux, M., Steig, E. J., Battisti, D. S., Johnson, N. C., Blanchard-Wrigglesworth, E., Po-Chedley, S., Zhang, Q., and Harnos, K.: Fingerprints of internal drivers of Arctic sea ice loss in observations and model simulations, *Nat. Geosci.*, 12, 28–33, 2019.
- Doherty, S. J., Dang, C., Hegg, D. A., Zhang, R., and Warren, S. G.: Black carbon and other light-absorbing particles in snow of central North America, *J. Geophys. Res.-Atmos.*, 119, 12807–12831, 2014.
- Doherty, S. J., Warren, S. G., Grenfell, T. C., Clarke, A. D., and Brandt, R. E.: Light-absorbing impurities in Arctic snow, *Atmos. Chem. Phys.*, 10, 11647–11680, <https://doi.org/10.5194/acp-10-11647-2010>, 2010.
- Dong, Z., Kang, S., Qin, D., Shao, Y., Ulbrich, S., and Qin, X.: Variability in individual particle structure and mixing states between the glacier–snowpack and atmosphere in the northeastern Tibetan Plateau, *The Cryosphere*, 12, 3877–3890, <https://doi.org/10.5194/tc-12-3877-2018>, 2018.
- Flanner, M. G., Zender, C. S., Randerson, J. T., and Rasch, P. J.: Present-day climate forcing and response from black carbon in snow, *J. Geophys. Res.*, 112, D11202, <https://doi.org/10.1029/2006JD008003>, 2007.
- Flanner, M. G., Liu, X., Zhou, C., Penner, J. E., and Jiao, C.: Enhanced solar energy absorption by internally-mixed black carbon in snow grains, *Atmos. Chem. Phys.*, 12, 4699–4721, <https://doi.org/10.5194/acp-12-4699-2012>, 2012.
- Grannas, A. M., Jones, A. E., Dibb, J., Ammann, M., Anastasio, C., Beine, H. J., Bergin, M., Bottenheim, J., Boxe, C. S., Carver, G., Chen, G., Crawford, J. H., Dominé, F., Frey, M. M., Guzmán, M. I., Heard, D. E., Helmig, D., Hoffmann, M. R., Honrath, R. E., Huey, L. G., Hutterli, M., Jacobi, H. W., Klán, P., Lefer, B., McConnell, J., Plane, J., Sander, R., Savarino, J., Shepson, P. B., Simpson, W. R., Sodeau, J. R., von Glasow, R., Weller, R., Wolff, E. W., and Zhu, T.: An overview of snow photochemistry: evidence, mechanisms and impacts, *Atmos. Chem. Phys.*, 7, 4329–4373, <https://doi.org/10.5194/acp-7-4329-2007>, 2007.
- Hadley, O. L. and Kirchstetter, T. W.: Black-carbon reduction of snow albedo, *Nat. Clim. Change*, 2, 437–440, 2012.
- He, C. L., Takano, Y., Liou, K. N., Yang, P., Li, Q., Chen, F., He, C., Takano, Y., Liou, K. N., and Yang, P.: Impact of Snow Grain Shape and Black Carbon-Snow Internal Mixing on Snow Optical Properties: Parameterizations for Climate Models, *J. Climate*, 30, 10019–10036, 2017.
- He, C., Flanner, M. G., Chen, F., Barlage, M., Liou, K.-N., Kang, S., Ming, J., and Qian, Y.: Black carbon-induced snow albedo reduction over the Tibetan Plateau: uncertainties from snow grain shape and aerosol–snow mixing state based on an updated SNICAR model, *Atmos. Chem. Phys.*, 18, 11507–11527, <https://doi.org/10.5194/acp-18-11507-2018>, 2018a.
- He, C. L., Liou, K. N., and Takano, Y.: Resolving Size Distribution of Black Carbon Internally Mixed With Snow: Impact on Snow Optical Properties and Albedo, *Geophys. Res. Lett.*, 45, 2697–2705, 2018b.
- He, C. L., Liou, K. N., Takano, Y., Yang, P., Qi, L., and Chen, F.: Impact of Grain Shape and Multiple Black Carbon Internal Mixing on Snow Albedo: Parameterization and Radiative Effect Analysis, *J. Geophys. Res.-Atmos.*, 123, 1253–1268, 2018c.
- Jacobson, M. Z.: Strong radiative heating due to the mixing state of black carbon in atmospheric aerosols, *Nature*, 409, 695–697, 2001.
- Kahnert, M., Nousiainen, T., Lindqvist, H., and Ebert, M.: Optical properties of light absorbing carbon aggregates mixed with sulfate: assessment of different model geometries for climate forcing calculations, *Opt. Express*, 20, 10042–10058, 2012.
- Kokhanovsky, A. A. and Zege, E. P.: Scattering optics of snow, *Appl. Optics*, 43, 1589–1602, 2004.
- Lack, D. A. and Cappa, C. D.: Impact of brown and clear carbon on light absorption enhancement, single scatter albedo and absorption wavelength dependence of black carbon, *Atmos. Chem. Phys.*, 10, 4207–4220, <https://doi.org/10.5194/acp-10-4207-2010>, 2010.
- Lack, D. A., Langridge, J. M., Bahreini, R., Cappa, C. D., Middlebrook, A. M., and Schwarz, J. P.: Brown carbon and internal mixing in biomass burning particles, *PNAS*, 109, 14802–14807, 2012.
- Li, X., Kang, S., He, X., Qu, B., Tripathee, L., Jing, Z., Paudyal, R., Li, Y., Zhang, Y., and Yan, F.: Light-absorbing impurities accelerate glacier melt in the Central Tibetan Plateau, *Sci. Total Environ.*, 587, 482–490, 2017.
- Li, X., Kang, S., Zhang, G., Qu, B., Tripathee, L., Paudyal, R., Jing, Z., Zhang, Y., Yan, F., and Li, G.: Light-absorbing impurities in a southern Tibetan Plateau glacier: Variations and potential impact on snow albedo and radiative forcing, *Atmos. Res.*, 200, 77–87, 2018.
- Liou, K. N., Takano, Y., and Yang, P.: Light absorption and scattering by aggregates: Application to black carbon and snow grains, *J. Quant. Spectrosc. Ra.*, 112, 1581–1594, 2011.
- Liou, K. N., Takano, Y., He, C., Yang, P., Leung, L. R., Gu, Y., and Lee, W. L.: Stochastic parameterization for light absorption by

- internally mixed BC/dust in snow grains for application to climate models, *J. Geophys. Res.-Atmos.*, 119, 7616–7632, 2014.
- Liu, D. T., Whitehead, J., Alfarrar, M. R., Reyes-Villegas, E., Spracklen, D. V., Reddington, C. L., Kong, S. F., Williams, P. I., Ting, Y. C., Haslett, S., Taylor, J. W., Flynn, M. J., Morgan, W. T., McFiggans, G., Coe, H., and Allan, J. D.: Black-carbon absorption enhancement in the atmosphere determined by particle mixing state, *Nat. Geosci.*, 10, 184–188, <https://doi.org/10.1038/ngeo2901>, 2017.
- Liu, J., Wu, D., Liu, G., Mao, R., Chen, S., Ji, M., Fu, P., Sun, Y., Pan, X., and Jin, H.: Impact of Arctic amplification on declining spring dust events in East Asia, *Clim. Dynam.*, 54, 1913–1935, 2020.
- Flanner, M. G., Liu, X., Zhou, C., Penner, J. E., and Jiao, C.: Enhanced solar energy absorption by internally-mixed black carbon in snow grains, *Atmos. Chem. Phys.*, 12, 4699–4721, <https://doi.org/10.5194/acp-12-4699-2012>, 2012.
- Matsui, H., Hamilton, D. S., and Mahowald, N. M.: Black carbon radiative effects highly sensitive to emitted particle size when resolving mixing-state diversity, *Nat. Commun.*, 9, 1–11, 2018.
- Meier, W. N., Hovelsrud, G. K., Van Oort, B. E., Key, J. R., Kovacs, K. M., Michel, C., Haas, C., Granskog, M. A., Gerland, S., and Perovich, D. K.: Arctic sea ice in transformation: A review of recent observed changes and impacts on biology and human activity, *Rev. Geophys.*, 52, 185–217, 2014.
- Moffet, R. C. and Prather, K. A.: In-situ measurements of the mixing state and optical properties of soot with implications for radiative forcing estimates, *PNAS*, 106, 11872–11877, 2009.
- Moteki, N., Kondo, Y., Miyazaki, Y., Takegawa, N., Komazaki, Y., Kurata, G., Shirai, T., Blake, D. R., Miyakawa, T., and Koike, M.: Evolution of mixing state of black carbon particles: Aircraft-measurements over the western Pacific in March 2004, *Geophys. Res. Lett.*, 34, L11803, <https://doi.org/10.1029/2006GL028943>, 2007.
- Peng, J. F., Hu, M., Guo, S., Du, Z. F., Zheng, J., Shang, D. J., Zamora, M. L., Zeng, L. M., Shao, M., Wu, Y. S., Zheng, J., Wang, Y., Glen, C. R., Collins, D. R., Molina, M. J., and Zhang, R. Y.: Markedly enhanced absorption and direct radiative forcing of black carbon under polluted urban environments, *P. Natl. Acad. Sci. USA*, 113, 4266–4271, 2016.
- Pu, W., Wang, X., Wei, H., Zhou, Y., Shi, J., Hu, Z., Jin, H., and Chen, Q.: Properties of black carbon and other insoluble light-absorbing particles in seasonal snow of northwestern China, *The Cryosphere*, 11, 1213–1233, <https://doi.org/10.5194/tc-11-1213-2017>, 2017.
- Pu, W., Cui, J., Shi, T., Zhang, X., He, C., and Wang, X.: The remote sensing of radiative forcing by light-absorbing particles (LAPs) in seasonal snow over northeastern China, *Atmos. Chem. Phys.*, 19, 9949–9968, <https://doi.org/10.5194/acp-19-9949-2019>, 2019.
- Qian, Y., Gustafson, W. I., Leung, L. R., and Ghan, S. J.: Effects of soot-induced snow albedo change on snowpack and hydrological cycle in western United States based on Weather Research and Forecasting chemistry and regional climate simulations, *J. Geophys. Res.-Atmos.*, 114, D03108, <https://doi.org/10.1029/2008JD011039>, 2009.
- Ramanathan, V. and Carmichael, G.: Global and regional climate changes due to black carbon, *Nat. Geosci.*, 1, 221–227, 2008.
- Ricchiazzi, P., Yang, S., Gautier, C., and Sowle, D.: SBDART: A research and teaching software tool for plane-parallel radiative transfer in the Earth's atmosphere, *B. Am. Meteorol. Soc.*, 79, 2101–2114, 1998.
- Schwarz, J. P., Gao, R. S., Perring, A. E., Spackman, J. R., and Fahey, D. W.: Black carbon aerosol size in snow, *Sci. Rep.*, 3, 1356, <https://doi.org/10.1038/srep01356>, 2013.
- Shi, T., Pu, W., Zhou, Y., Cui, J., Zhang, D., and Wang, X.: Albedo of Black Carbon-Contaminated Snow Across Northwestern China and the Validation With Model Simulation, *J. Geophys. Res.-Atmos.*, 125, e2019JD032065, <https://doi.org/10.1029/2019JD032065>, 2020.
- Sun, H. L., Biedermann, L., and Bond, T. C.: Color of brown carbon: A model for ultraviolet and visible light absorption by organic carbon aerosol, *Geophys. Res. Lett.*, 34, L17813, <https://doi.org/10.1029/2007GL029797>, 2007.
- Toon, O. B., McKay, C. P., Ackerman, T. P., and Santhanam, K.: Rapid Calculation of Radiative Heating Rates and Photodissociation Rates in Inhomogeneous Multiple-Scattering Atmospheres, *J. Geophys. Res.-Atmos.*, 94, 16287–16301, 1989.
- Turpin, B. J. and Lim, H. J.: Species contributions to PM_{2.5} mass concentrations: Revisiting common assumptions for estimating organic mass, *Aerosol Sci. Tech.*, 35, 602–610, 2001.
- Wang, X., Doherty, S. J., and Huang, J.: Black carbon and other light-absorbing impurities in snow across Northern China, *J. Geophys. Res.-Atmos.*, 118, 1471–1492, 2013.
- Wang, X., Pu, W., Ren, Y., Zhang, X., Zhang, X., Shi, J., Jin, H., Dai, M., and Chen, Q.: Observations and model simulations of snow albedo reduction in seasonal snow due to insoluble light-absorbing particles during 2014 Chinese survey, *Atmos. Chem. Phys.*, 17, 2279–2296, <https://doi.org/10.5194/acp-17-2279-2017>, 2017.
- Warren, S. G. and Wiscombe, W. J.: A Model for the Spectral Albedo of Snow. 2: Snow Containing Atmospheric Aerosols, *J. Atmos. Sci.*, 37, 2734–2745, 1980.
- Xu, B. Q., Cao, J. J., Hansen, J., Yao, T. D., Joswila, D. R., Wang, N. L., Wu, G. J., Wang, M., Zhao, H. B., Yang, W., Liu, X. Q., and He, J. Q.: Black soot and the survival of Tibetan glaciers, *PNAS*, 106, 22114–22118, 2009.
- Yang, M., Howell, S. G., Zhuang, J., and Huebert, B. J.: Attribution of aerosol light absorption to black carbon, brown carbon, and dust in China – interpretations of atmospheric measurements during EAST-AIRE, *Atmos. Chem. Phys.*, 9, 2035–2050, <https://doi.org/10.5194/acp-9-2035-2009>, 2009.
- Yao, T. D., Thompson, L., Yang, W., Yu, W. S., Gao, Y., Guo, X. J., Yang, X. X., Duan, K. Q., Zhao, H. B., Xu, B. Q., Pu, J. C., Lu, A. X., Xiang, Y., Kattel, D. B., and Joswiak, D.: Different glacier status with atmospheric circulations in Tibetan Plateau and surroundings, *Nat. Clim. Change*, 2, 663–667, 2012.
- Ye, H., Zhang, R., Shi, J., Huang, J., Warren, S. G., and Fu, Q.: Black carbon in seasonal snow across northern Xinjiang in northwestern China, *Environ. Res. Lett.*, 7, 044002, <https://doi.org/10.1088/1748-9326/7/4/044002>, 2012.
- You, R., Radney, J. G., Zachariah, M. R., and Zangmeister, C. D.: Measured Wavelength-Dependent Absorption Enhancement of Internally Mixed Black Carbon with Absorbing and Nonabsorbing Materials, *Environ. Sci. Technol.*, 50, 7982–7990, 2016.
- Zhang, Y., Kang, S., Cong, Z., Schmale, J., Sprenger, M., Li, C., Yang, W., Gao, T., Sillanpää, M., and Li, X.: Light-absorbing im-

purities enhance glacier albedo reduction in the southeastern Tibetan Plateau, *J. Geophys. Res.-Atmos.*, 122, 6915–6933, 2017.

Zhang, Y., Kang, S., Sprenger, M., Cong, Z., Gao, T., Li, C., Tao, S., Li, X., Zhong, X., Xu, M., Meng, W., Neupane, B., Qin, X., and Sillanpää, M.: Black carbon and mineral dust in snow cover on the Tibetan Plateau, *The Cryosphere*, 12, 413–431, <https://doi.org/10.5194/tc-12-413-2018>, 2018.